ELSEVIER

Journal of Organometallic Chemistry 550 (1998) 141–150

Journal of Organometallic Chemistry

The non-perpendicular and non-parallel alkyne bridge in $W_2(\mu\text{-}C_2H_2)(\mu\text{-}OCH_2^tBu)_2(OCH_2^tBu)_6$ [1]

Malcolm H. Chisholm, Matthew A. Lynn *

Department of Chemistry, Indiana University, Bloomington, IN 47405, USA

Received 3 February 1997

Abstract

The bonding in the ethyne adduct $W_2(\mu\text{-}C_2H_2)(\mu\text{-}ONp)_2(ONp)_6$ (Np = CH_2^tBu) has been examined by various computational methods [Extended Hückel (EHMO), Fenske–Hall, and Gaussian 92 RHF (Restricted Hartree–Fock) and density functional (Becke-3LYP) calculations] employing the model compound $W_2(\mu\text{-}C_2H_2)(\mu\text{-}OH)_2(OH)_6$. EHMO and Fenske–Hall calculations suggest, based on *total* orbital energy, that a μ-parallel ethyne geometry should have the lowest energy, although traditional frontier orbital arguments agree with the observance of a skewed acetylene bridge. Gaussian 92 computations reproduce the non-perpendicular/non-parallel $\mu\text{-}C_2H_2$ geometry in close agreement to that observed in the solid-state (X-ray) structure, which leads us to suggest that the distortion is not sterically imposed by the attendant alkoxide ligands. The observed geometry can be rationalized in terms of Jahn–Teller distortional stabilization from either the μ-parallel or μ-perpendicular mode, i.e., the geometry is favored on electronic grounds, though the potential energy surface is rather shallow. These results are discussed in terms of previous studies of the addition of alkynes to d^3–d^3 dinuclear complexes of tungsten and in terms of relationships between d^2-$W(OR)_4$ and d^8-$Os(CO)_4$ fragments. © 1998 Elsevier Science S.A.

Keywords: Tungsten; Alkyne bridge; Total orbital energy

1. Introduction

One of the most powerful techniques in understanding the electronic structures of organometallic compounds, including clusters, is the fragment molecular orbital approach. In a pseudo-retrosynthetic procedure, a molecule is broken apart and viewed as the combination of various fragments. The advantage this approach offers is that the molecular moieties can be chosen such that these frontier molecular orbitals and their electron occupation are readily recognizable. Two fragments may be viewed as isolobal when their frontier molecule orbitals are of the same symmetry, they have the same electron count and a similar match in energy [1]. In this way Hoffmann taught us to look for relationships between organic, organometallic and inorganic complexes [2]. In our research we have found it useful to consider the d^3-$W(OR)_3$ fragment isolobal with CR, P, As, and $Co(CO)_3$ [3]. The compounds $(RO)_3WW(OR)_3$ are inorganic analogues of alkynes; $W_2(OR)_6(\mu\text{-}C_2R'_2)(py)_n$ where $n = 1$ or 2, are dimetallatetrahedranes and complexes of the formula $W_3(OR)_9(\mu^3\text{-}X)$ where X = CR′ or P are related to the carbonyl clusters $Co_3(CO)_9(\mu_3\text{-}X)$ where X = CR′ or P [3].

The d^2-$W(OR)_4$ fragment may be viewed as isolobal with the d^8-$Os(CO)_4$ fragment because each has one frontier orbital of σ-type symmetry and one of π; the total electron occupation of the fragment orbitals of the tungsten-containing moiety is, of course, two. The complexes $W_2(OR)_8$ and $Os_2(CO)_8$ each have M–M double bonds and are labile toward associative chemistry. It is well known from the pioneering work of Takats that alkynes add to $Os_2(CO)_8$ to give μ-parallel alkyne complexes, organometallic analogues of cyclobutenes [4]. Similarly, from many elegant studies by Bullock et al. [5], and Hembre et al. [6] it has been shown that ethylene and $Os_2(CO)_8$ combine in a 2 + 2 manner to give dimetallacyclobutanes. It was then of some surprise to us to find that $W_2(OCH_2^tBu)_8$ reacted with ethyne, ethene, allene and carbon monoxide to give products whose structures were not readily accountable

* Corresponding author. Department of Chemistry, University of Arizona, Tucson, AZ 85721, USA.

[1] Dedicated to Professor Ken Wade, FRS, on the occasion of his 65th birthday.

in terms of expectations based on the isolobal relationship between d^2-$W(OR)_4$ and d^8-$Os(CO)_4$ [7]. In this paper we examine in detail the bonding in the ethyne adduct $W_2(\mu\text{-}C_2H_2)(\mu\text{-}ONp)_2(ONp)_6$, which has a distinctly non-perpendicular and non-parallel mode of bonding. As Hoffman and Hoffmann noted, this is a relatively rare occurrence in ethyne bridged metal complexes.

2. Computational procedure

We start by reducing the molecule to the more computationally manageable $W_2(\mu\text{-}OH)_2(OH)_6(\mu\text{-}C_2H_2)$ hypothetical molecule. With a $W_2(\mu\text{-}OH)_2(OH)_6$ template frozen into the observed $W_2(\mu\text{-}OC)_2(OC)_6$ framework found in the solid-state structure, shown in Fig. 1, we explore the ethyne interactions by EHMO and Fenske–Hall procedures. Then we employ ab inito calculations to optimize the geometry of a $W_2(\mu\text{-}OH)_2(OH)_6(\mu\text{-}C_2H_2)$ molecule and ultimately return to see a simple explanation of why neither a parallel or perpendicular mode of bonding is favored.

The structure for the hypothetical compound $W_2(\mu\text{-}C_2H_2)(\mu\text{-}OH)_2(OH)_6$ was taken from the crystal structure of $W_2(\mu\text{-}C_2H_2)(\mu\text{-}ONp)_2(ONp)_6$ [7]. Because the C–C–H angle is not available from the crystallographic data, calculations in which the acetylene fragment is rotated above $W_2(\mu\text{-}OH)_2(OH)_6$ were performed for $\angle_{C-C-H} = 120°$, 150°, and 180°. The symmetries of the $W_2(\mu\text{-}OH)_2(OH)_6$ and C_2H_2 fragments were maintained at C_{2v} throughout the rotations; at angles of rotation between 0° and 90°, the structure possesses C_2 symmetry. At the parallel and perpendicular orientations, of course, the structure has C_{2v} symmetry.

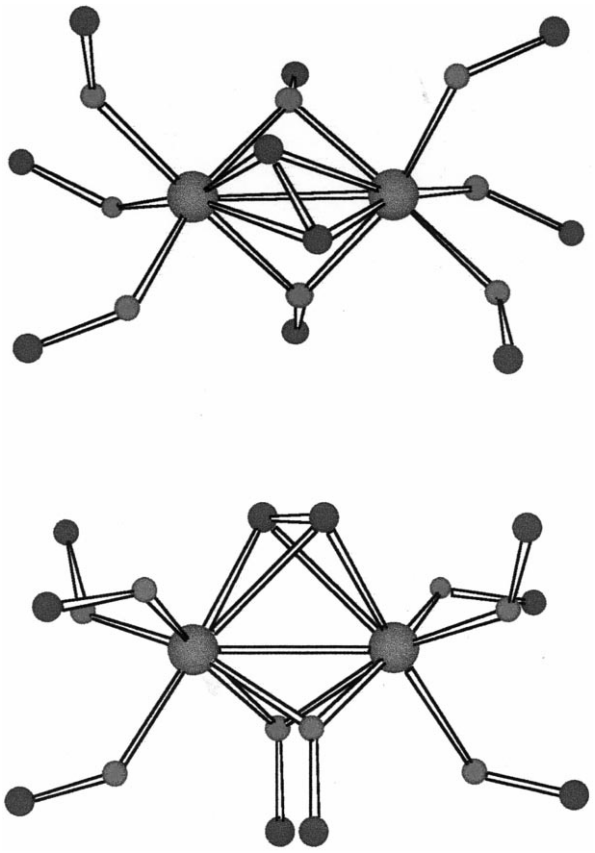

Fig. 1. Top and side views of the $W_2(\mu\text{-}OC)_2(OC)_6(\mu\text{-}C_2H_2)$ core of $W_2(\mu\text{-}C_2H_2)(\mu\text{-}ONp)_2(ONp)_6$.

Fenske–Hall molecular orbital calculations [8] were performed at the Indiana University Computational Chemistry Center on the UCS STARRS (Scalar Technology Array of Risc-Based Research Systems) system, which comprises 15 IBM Risc System/6000 POWERservers of various models. Atomic basis functions were generated using the method of Bursten et al. [9]. Contracted double-zeta functions were used for the W 5d atomic orbitals and for the carbon and oxygen 2p atomic orbitals. Basis functions for tungsten were derived for the 1 + oxidation state with the valence s and p exponents fixed at 2.4 for the W 6s and 6p orbitals. Ground state atomic configurations were used for the basis functions of all other atoms. An exponent of 1.20 was used for the H 1s AO. Extended Hückel calculations were performed with the CACAO computational package [10]. The ordering of the frontier molecular orbitals by the EHMO calculations is the same as predicted by the Fenske–Hall calculations and will not be discussed separately.

For the Gaussian 92 geometry optimizations [11], the starting structure was taken from the crystallographic data report. To confirm the twisted orientation of the acetylene moiety, geometry optimizations were begun with the C_2H_2 fragment in various torsional angles. During optimizations, the structure was required to possess at least C_2 symmetry. For this system, an effective core potential (ECP) was employed for W, using the 5d6s6p valence space. The ECP of Ross et al. was chosen with a (3s3p4d) Gaussian basis set contracted into [111/111/211] [12]. For O and C, (9s5p) Gaussian basis sets were contracted into [6111/41] and were augmented by a d polarization function ($\zeta = 1.0$) [13]. For the H atoms, a (4s) Gaussian basis set contracted into the [1s] basis set of Huzinaga was used [14]. Geometry optimizations were performed at the RHF and Becke3LYP (density functional) levels.

3. Background

The molecular structures such dimetal complexes exhibit upon uptake of a small molecule substrate have generated much interest among computational chemists. One example is the series obtained when acetylene

Fig. 2. Parallel and perpendicular orientations of acetylene-bridged dimers.

(C_2H_2) and related derivatives are taken up by organometallic/metalloorganic species. Many μ-C_2H_2 complexes adopt so-called 'parallel' and 'perpendicular' structures in which the CRC and M–M bond axes are related by dihedral angles of 0° and 90°, respectively, as shown in Fig. 2.

Initial molecular orbital arguments for the preference of parallel or perpendicular C_2R_2 arrangements were based on the metal-acetylene valence orbital interactions. The important fragment orbitals of the C_2 unit are the two highest occupied and two lowest unoccupied. Of course, before coordination of the acetylene to the metal dimer, the C_2 unit has a filled, doubly degenerate set of C–C π bonds and an unfilled degenerate set of C–C π^* antibonds. Upon coordination of the ethyne moiety, the C–C bond order is reduced by donation of electrons from the C–C π fragment orbital (FO) and acceptance of electron density into the CRC π^* FO and the C–C–R bond angle decreases from 180° to between 120° and 150°; the hybridization around the carbon atoms can thus be thought of as changing from sp to sp^2. The π and π^* orbitals that are perpendicular to the H–C–C–H plane are unperturbed by the closing of the C–C–R angle. The other π and π^* orbitals, however, are pushed away from inside the C–C–R angle; the π bond becomes less bonding and is destabilized while the π^* antibond becomes less antibonding and is stabilized relative to the other π^* C–C FO.

The resulting valence orbitals of the C_2R_2 moiety are thus available for bonding in the well-known Dewar–Chatt–Duncanson fashion, in which bonding between two fragments occurs via a synergistic exchange of electrons between symmetry-appropriate orbitals of the two units. Mixing of metal- and acetylene-based frontier orbitals gives the molecular orbitals shown in Fig. 3 for a C_2R_2 moiety in the parallel arrangement. Similar donor-acceptor interactions also occur when the acetylene bridge is oriented in the perpendicular position. Molecular orbital arguments for the preference of either parallel or perpendicular orientations have been based on orbital (i.e., symmetry-allowedness) and energy match criteria. Depending on the electron count of the dimetallic species, some or all of the orbital interactions shown in Fig. 3 will be occupied, either completely or partially, or empty.

Hoffmann et al. [15] have probed the frontier orbital differences when the acetylene bridge is rotated from perpendicular to parallel in a variety of C_2R_2-bridged species. The argument for a perpendicular acetylene geometry for this molecule lies in the interactions allowed by symmetry between the C_2H_2 and $Co_2(CO)_6$ moities. For $\Theta = 90°$, the filled acetylene orbitals of a_1 and b_2 symmetry interact, respectively, with the empty $2a_1$ and $1b_2$ fragment orbitals of $Co_2(CO)_6$. In addition, the metal fragment backbonds to the acetylene as its filled orbitals $1a_2$ and $1b_1$ interact with the empty a_2 and b_1 C_2H_2 orbitals, respectively. Rotating the acetylene bridge to the parallel orientation destroys two of these four bonding interactions. That is, whereas two C_2H_2 orbitals were able to donate to the metal fragment and two $Co_2(CO)_6$ orbitals had the ability to backbond to the acetylene fragment, rotating the C_2H_2 moiety gives rise to a destabilizing interaction between the filled b_1 orbital of C_2H_2 and the filled $1b_1$ orbital of $Co_2(CO)_6$. Note that, because of the location of the plane of symmetry with respect to the acetylene fragment in the two positions, the acetylene fragment orbitals of b_1 symmetry in the perpendicular orientation possess b_2 symmetry in the parallel position and vice versa. Additionally, the unfilled b_2 acetylene orbital can only mix with the unfilled $1b_2$ $Co_2(CO)_6$ frontier or-

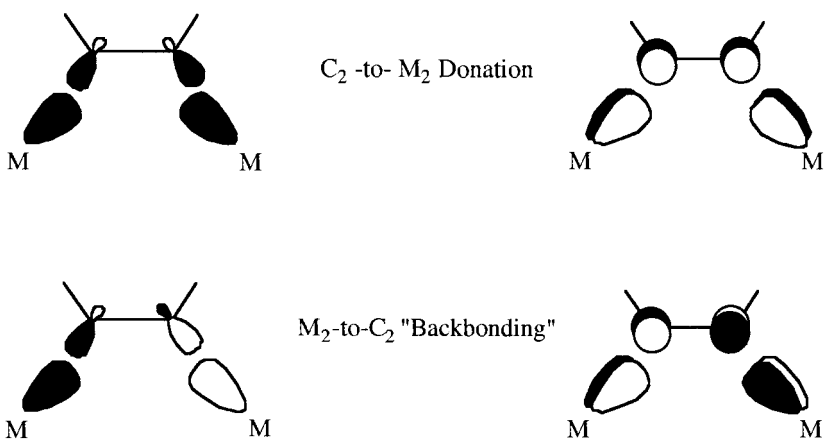

Fig. 3. Metal–acetylene bonding orbital combinations.

bital. Essentially, two molecular orbitals that were bonding in the perpendicular orientation have become one filled–filled repulsion and one unfilled–unfilled nonbonding interaction when the acetylene fragment is placed in a parallel fashion.

As might be expected, not all bridging acetylene complexes display a C_2H_2 fragment in a parallel or perpendicular fashion. Workers in our laboratories [16] demonstrated with the crystal structure of $W_2(\mu\text{-}NMe_2)_2(\mu\text{-}C_2Me_2)Cl_4(py)_2$ that the C_2 moiety can be found between these two extremes; the plane of the C_2Me_2 fragment is rotated 55° from the W–W bond axis. Calhorda and Hoffmann responded with an Extended Hückel treatment of the system [17]. These authors invoked a second-order Jahn–Teller distortion argument in which at $\Theta = 90°$, a small HOMO–LUMO gap is observed and determined that the energy difference between these two orbitals can be maximized if the C_2 unit is rotated to an angle of 135°. The molecular orbital diagram proposed by Calhorda and Hoffmann for the related but hypothetical complex $W_2(\mu\text{-}NH_2)_2(C_2H_2)Cl_6^{2-}$ is shown in Fig. 4; the orbital labels are for C_{2v} symmetry.

As the acetylene unit is rotated from parallel or perpendicular, the symmetry of the system is lowered to C_2 and all $W_2(\mu\text{-}NH_2)_2Cl_6^{2-}$ and C_2H_2 fragment orbitals that originally had a_1 or a_2 symmetry can mix as can those originally of b_1 or b_2 symmetry. As a consequence, the HOMO (orbital $3a_1$ at $\Theta = 90°$) of $W_2(\mu\text{-}NH_2)_2(C_2H_2)Cl_6^{2-}$ is stabilized; the second highest unoccupied acetylene orbital (π^* a_2 at $\Theta = 90°$) is now allowed by symmetry to interact with it. The LUMO ($1a_2$) of the complex is destabilized as the bonding interaction between the metal-centered fragment orbital $2a_1$ and acetylene orbital a_2 is weakened.

Several papers using similar orbital arguments have appeared in the literature since Calhorda and Hoffmann's account. Cotton and Feng [18] examined the structures of $Nb_4Cl_4O(PhCCPh)(THF)_4$, $W_2Cl_4(NMe_2)_2(\mu\text{-}MeCCMe)(py)_2$, $[Mo_2(\mu\text{-}4\text{-}MeC_6H_4CCH)(\mu\text{-}O_2CMe)(en)_4]^{3+}$, and $Ta_2Cl_6(Me_3CCCCMe_3)(THF)_2$ with the SCF-X α-SW method and used HOMO–LUMO energy gap criteria to determine whether or not the alkyne bridges in these systems should adopt perpendicular, parallel, or skewed orientations. Aggarwal et al. [19], in another work, provided experimental evidence to the alkyne rotation predicted by Thorn and Hoffmann [20] upon the one-electron oxidation of the complexes $Co_2(CO)_2(\mu\text{-}RC_2R)(\mu\text{-}dppm)_2$. Bott et al. gave a more complete theoretical description of the bonding in $W_2Cl_4(\mu\text{-}Cl)_2(\mu\text{-}C_2R_2)thf)_2$ in which they suggested that the tight metal-μ-alkyne bonding in such a complex can suppress a possible second-order Jahn–Teller distortion because of an already large HOMO–LUMO gap [21]. In a subsequent account, Mountford [22] proposed that the skewed placement of C_2Ph_2 in $W_2(\eta\text{-}C_5H_4Pr^i)_2Br_4(\mu\text{-}C_2Ph_2)$ is not a result of a second-order Jahn–Teller distortion because the HOMO and LUMO cannot mix as the symmetry of the system is lowered; the LUMO has b symmetry whereas the HOMO is of a symmetry. Rather, the $[W_2(\eta\text{-}C_5H_5)_2Br_4]$ moiety adopts a geometry analogous to a staggered

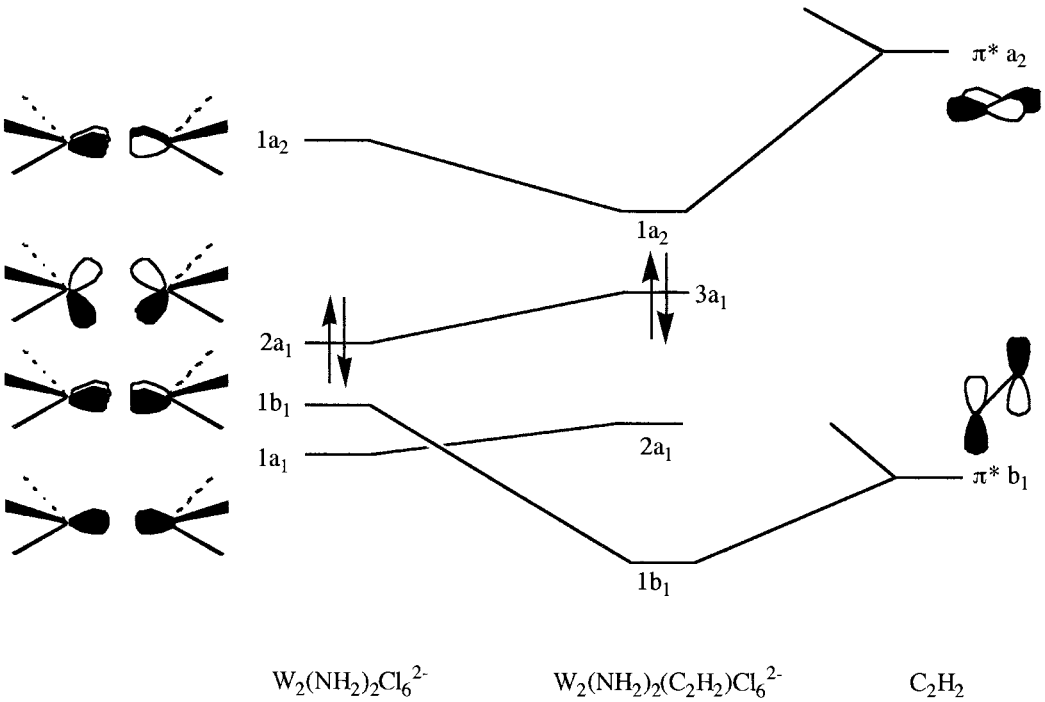

Fig. 4. Abbreviated molecular orbital diagram of Calhorda and Hoffmann for $W_2(\mu\text{-}NH_2)_2(C_2H_2)Cl_6^{2-}$.

ethane because there is little metal-to-acetylene back-bonding to lose by rotation. The resulting valence fragment orbitals of the ditungsten system support a skewed acetylene fragment.

The recent synthesis and subsequent structural determination of $W_2(\mu\text{-}C_2H_2)(\mu\text{-}ONp)_2(ONp)_6$ has shown that the acetylene bridge is twisted from the W–W bond axis very much as the C_2H_2 fragment is turned in the structure reported by Ahmed et al. A molecular orbital study of the system is therefore appropriate. However, even before calculations are performed, it is possible to make several observations regarding this system. First the electronic explanation is most likely not similar to that of Mountford because all of the terminal ligands (namely, neopentoxides) are the same, analogous to the $W_2(\mu\text{-}NH_2)_2(C_2H_2)Cl_6^2$ system examined by Calhorda and Hoffmann. Second, in $W_2(\mu\text{-}NH_2)_2(C_2H_2)Cl_6^{2-}$, the electron count at the metal atoms is d^2–d^2 (assuming the acetylene fragment can be considered as $C_2H_2^{2-}$), but in the molecule of current interest the count is d^1–d^1. Therefore, although it might appear that the removal of two electrons from Calhorda and Hoffmaun's bonding scheme should give the correct molecular orbital diagram for $W_2(\mu\text{-}C_2H_2)(\mu\text{-}ONp)_2(ONp)_6$, a second-order Jahn–Teller argument would be neither expected nor valid based on this predicted electronic structure. The HOMO of $W_2(\mu\text{-}NH_2)_2(C_2H_2)Cl_6^{2-}$, which was stabilized upon twisting of C_2H_2, would be the LUMO for $W_2(\mu\text{-}C_2H_2)(\mu\text{-}ONp)_2(ONp)_6$; stabilization of the LUMO is counterintuitive to the Jahn–Teller distortion argument. Finally, such orbital arguments seem to imply that the twist is not induced by steric influence of the attendant ligands, but it can certainly be argued that the Extended Hückel and similar methods were not designed to be geometry optimization tools. Therefore, this molecular study of the electronic structure of $W_2(\mu\text{-}C_2H_2)(\mu\text{-}ONp)_2(ONp)_6$ employs Fenske–Hall molecular orbital calculations to relate this system to previous orbital studies and Gaussian 92 geometry optimizations of various levels of computational sophistication to lend credibility to the belief that such a distortion of a bridging alkyne is not steric-induced.

4. Results and discussion

Once the acetylene fragment has been rotated atop the $W_2(\mu\text{-}OH)_2(OH)_6$ fragment with varying C–C–H angles, the energies of the various occupied and unoccupied molecular orbitals demonstrate that a second-order Jahn–Teller distortion in which the acetylene fragment rotates away from the perpendicular orientation is certainly possible, despite the concerns related in correlating Calhorda and Hoffmann's MO picture with the current system's electron count. A Walsh diagram

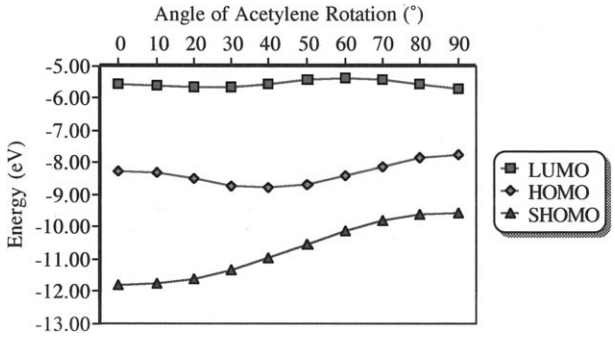

Fig. 5. Walsh diagram of the LUMO (a_2), HOMO (a_1), and SHOMO (b_2 at 90°, b_1 at 0°) energies vs. acetylene twist angle for $W_2(\mu\text{-}C_2H_2)(\mu\text{-}OH)_2(OH)_6$.

of the LUMO, HOMO, and SHOMO energies is presented in Fig. 5 and the HOMO–LUMO energetic gap vs. acetylene twist angle is shown in Fig. 6. Contour plots of the HOMO and LUMO at $\Theta = 0°$ are presented in Fig. 7.

As expected from the d^1–d^1 electronic configuration, the HOMO of the system is the W–W d_{z2} σ bond. The LUMO is a W–W π^*/δ^* hybrid and is tungsten–acetylene π bonding. It is easy to see why the LUMO is destabilized upon rotation of the C_2H_2 fragment; the W–C bonds are broken as the acetylene is turned toward $\Theta \approx 60°$ at which point the W–C bonds reform as Θ approaches 90°. A contour plot, shown in Fig. 8, of the HOMO at $\Theta = 60°$ shows why this MO is stabilized upon twisting of the fragment. Essentially, the out-of-plane acetylene π^* antibond can bond with the tori of the W d_{z2} σ bond. The stronger the metal–acetylene bonding, the more the molecular orbital is energetically stabilized as can be seen from Fig. 9 in which the metalacetylene (W d_{z2} σ bond-acetylene a_2 π^*) overlap and the energy of the HOMO are presented as functions of the angle of acetylene rotation.

Similarly, the LUMO is destabilized as the acetylene fragment is rotated away from 0° or 90°, as shown in Fig. 10. Note that the LUMO is most destabilized at $\Theta = 60°$ and that the energies of the LUMO at $\Theta = 0°$ and 90° are similar because the metal-C_2 π^* interac-

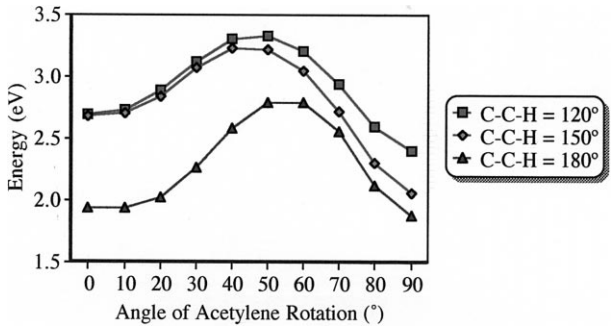

Fig. 6. HOMO–LUMO gap vs. acetylene twist angle for $W_2(\mu\text{-}C_2H_2)(\mu\text{-}OH)_2(OH)_6$.

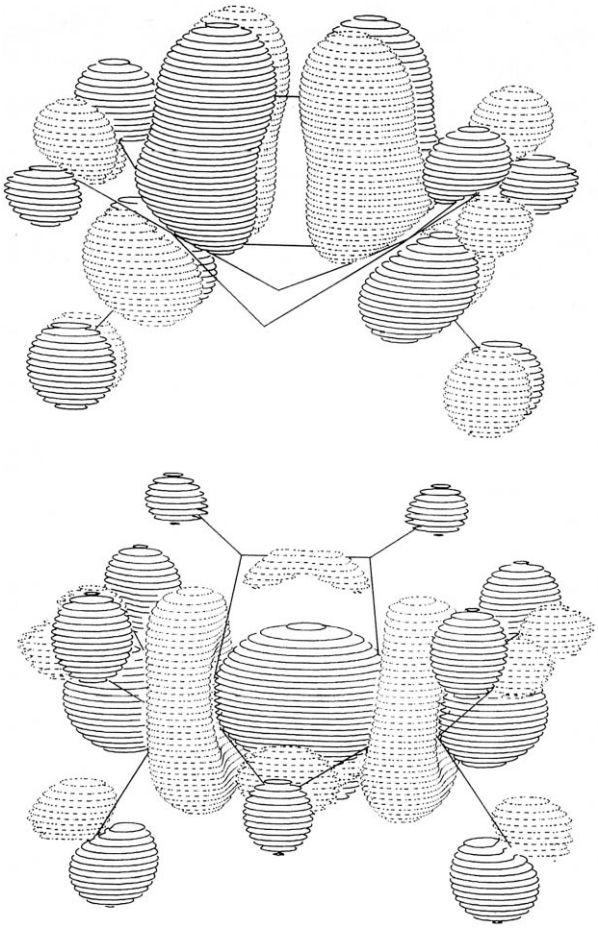

Fig. 7. Contour plots of the HOMO (bottom) and LUMO (top) of $W_2(\mu\text{-}C_2H_2)(\mu\text{-}OH)_2(OH)_6$ at $\Theta = 0°$.

tions are the same. That is, the metal- and acetylene-based fragment orbitals of which this MO is composed both possess a_2 symmetry at $\Theta = 0°$ and 90° Obviously, the minimum in metal-acetylene overlap and the maximum in the energy of the LUMO are not as coincident as were the overlap maximum and HOMO energy in Fig. 9. However, in Fig. 11, a plot of the total acetylene character found in the LUMO and the metal-acetylene overlap vs. the angle of acetylene rotation shows a slightly better agreement between the two functions.

Although a second-order Jahn–Teller distortion is usually simply described as occurring when the LUMO is most destablized, the HOMO is most stabilized, and both have the same reduced symmetry, implicit in this argument is the ability of the fragment orbitals that form these MO's to mix. The out-of-plane C–C π^* orbital at $\Theta = 90°$ is by symmetry only found in the molecule's LUMO because it and the rest of the MO possess a_2 symmetry. At $\Theta = 90°$, the C–C π^* fragment orbital cannot interact by symmetry with the W–W σ bond, which possesses a_1 symmetry. However, as soon as the acetylene fragment is turned, the out-of-plane C–C π^* fragment orbital can interact with the W–W d_{z2} σ bond, thereby stabilizing the HOMO. Because the symmetry of the molecule has been lowered to C_2 from C_{2v}, orbitals are only symmetric or antisymmetric with respect to the axis of rotation; any fragment orbital that has a symmetry can mix as can any with b symmetry, provided that energy and overlap requirements are met.

By examining the frontier MO's of this system, it seems clear that a second-order Jahn–Teller distortion is to be expected. However, it is not immediately clear why the LUMO found by Calhorda and Hoffmann is also the LUMO found for a system with two less electrons. At first thought, it might appear that using a different computational method with different basis functions than used by Calhorda and Hoffmann might be responsible for the difference. However, it is probably best to examine the structures used by Calhorda and Hoffmann for $W_2(\mu\text{-}NH_2)_2Cl_6(C_2H_2)^{2-}$ and here for $W_2(\mu\text{-}C_2H_2)(\mu\text{-}OH)_2(OH)_6$. In terms of fragment orbitals, the attendant ligands in both systems are quite similar. In the former case, the terminal ligands are chlorides and in the latter they are alkoxides, but both have essentially two p_π lone pairs and one p_σ lone pair. However, there is quite a difference in W–W bond distances, as would be expected from the predicted difference in formal bond orders: $W_2(\mu\text{-}NH_2)_2Cl_6(C_2H_2)^{2-}$, 2.436 Å; $W_2(\mu\text{-}C_2H_2)(\mu\text{-}OH)_2(OH)_6$, 2.623 Å. Therefore, to verify the method and to understand the differences in valence electronic structure, additional Fenske–Hall calculations have been performed on the following systems: $W_2(\mu\text{-}C_2H_2)(\mu\text{-}OH)_2(OH)_6^{2-}$ with a W–W distance of 2.436 Å and $W_2(\mu\text{-}C_2H_2)(\mu\text{-}OH)_2(OH)_6$ with the same bond distance. A qualitative correlation diagram summarizing these results is presented in Fig. 12.

For the structure with the shortened distance, the center of the C–C bond was moved to 1.87 Å above the W–W bond, which is the distance used by Calhorda and Hoffmann. The most notable results of these calculations are: (1) the frontier molecular orbital configuration is the same as predicted by Calhorda and Hoffmann

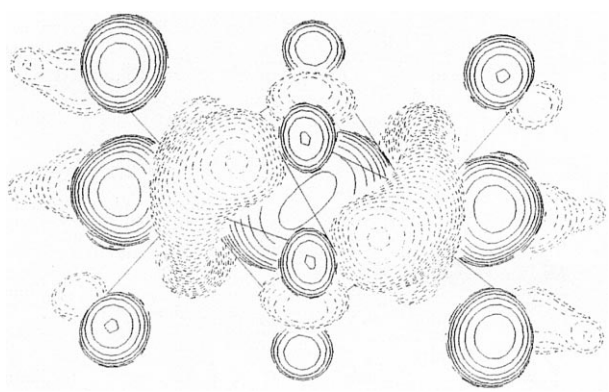

Fig. 8. Contour plot of the HOMO of $W_2(\mu\text{-}C_2H_2)(\mu\text{-}OH)_2(OH)_6$ at $\Theta = 60°$.

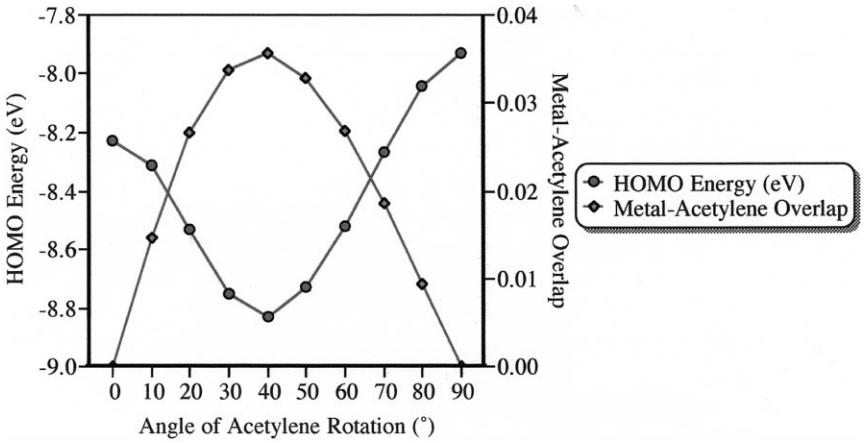

Fig. 9. Metal–acetylene overlap and energy of the HOMO vs. acetylene twist angle.

when the W–W distance is 2.436 Å and two electrons are added to the system; and (2) removing two electrons from $W_2(\mu\text{-}C_2H_2)(\mu\text{-}OH)_2(OH)_6^{2-}$ but maintaining the shorter distance gives rise to an MO configuration in which the HOMO of the dinegative species is the LUMO of the neutral compound. However, subsequent elongation of the metal–metal bond raises the energy of the LUMO of the uncharged complex above that of the next highest unoccupied MO. The reason for the switch in relative energies of the lowest two unoccupied MO's upon W–W bond elongation is that at the shortened W–W distance, the SLUMO (second lowest unoccupied molecular orbital) is an MO that is W_2-to-C_2H_2 bonding but strongly metal–metal antibonding (W–W π^*/δ^*) in character whereas the LUMO is W–W bonding akin to orbital $3a_1$ in Calhorda and Hoffman's diagram. The metal–acetylene bonding component of the SLUMO is not strong enough to overcome the W–W π^*/δ^* character of the bond at the shortened distance. However, as the bond order is lowered, the metal–metal bond distance increases, and the metal–metal antibonding character of this bond is diminished. The tungsten–acetylene bonding character is strong enough to lower the energy of this bond such that this molecular orbital is the LUMO at longer W–W distances. At the same time, the lengthening of the W–W bond decreased the metal–metal bonding nature of the former LUMO and this MO is raised in energy. Described in terms of Calhorda and Hoffmann's MO diagram shown in Fig. 4, the W–W d_{z2} σ bond (orbital $2a_1$) is the predicted HOMO as two electrons are removed from the system and orbital $1a_2$ (the tungsten–acetylene backbonding MO) drops below orbital $3a_1$ as it is stabilized upon elongation of the W–W bond.

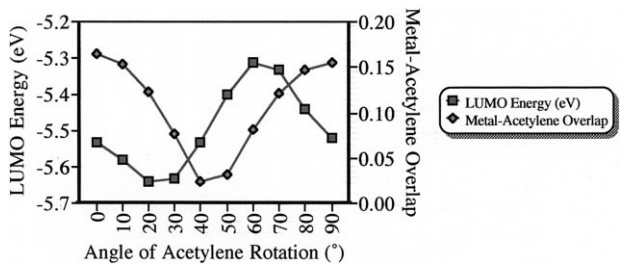

Fig. 10. Metal–acetylene overlap and energy of the LUMO vs. acetylene twist angle.

A final test of this qualitative MO argument is a comparison of the twist angles found in $W_2(\mu\text{-}NMe_2)_2(\mu\text{-}C_2Me_2)Cl_4(py)_2$ and $W_2(\mu\text{-}ONp)_2(ONp)_6(C_2H_2)$: 55° in the former and 63° in the latter. The similarity between the two attests to the similar molecular orbitals used to explain the Jahn–Teller distortion.

To test the hypothesis that the acetylene twist is not due to steric factors, Gaussian 92 geometry optimizations have been performed. Despite changing the computational method and the valence basis functions of the tungsten atoms, three separate calculations confirm that a twisted configuration is energetically favored when hydroxide groups are used in place of the more bulky neopentoxide substituents. Shown in Fig. 13 are top and side views of the RHF optimized structure for $W_2(\mu\text{-}C_2H_2)(\mu\text{-}OH)_2(OH)_6$ with movable bridging hydroxides. Various structural parameters and their actual and optimized values are presented in Table 1.

Of course, the most desired value in this series of optimized parameters is the rotation angle of acetylene. All the calculations find this torsional angle to be near the crystallographically determined value of 63.4°. The modeling of the relatively large neopentoxide groups with hydroxides and the proximity of the calculated angle of acetylene rotation supports the belief that the skewed nature of the C_2H_2 fragment in this molecule is a result of electronic, rather than steric, effects.

Also of prime interest in these values are the calculated W–W and C–C bond distances and the C–C–H bond angle, as these suggest the degree to which the acetylene fragment is bound to the metal-alkoxide core.

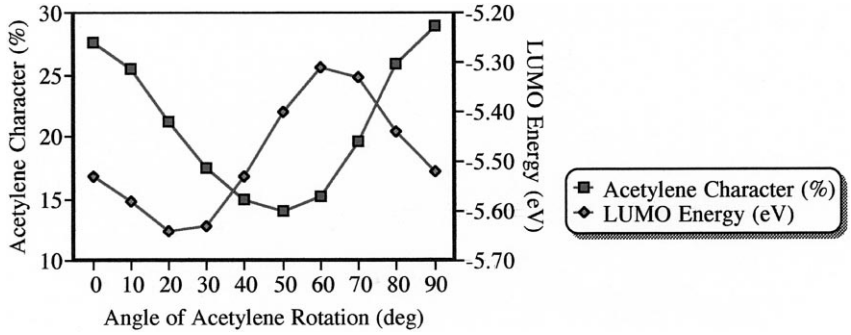

Fig. 11. Plot of total acetylene character in the LUMO and LUMO energy vs. angle of acetylene rotation.

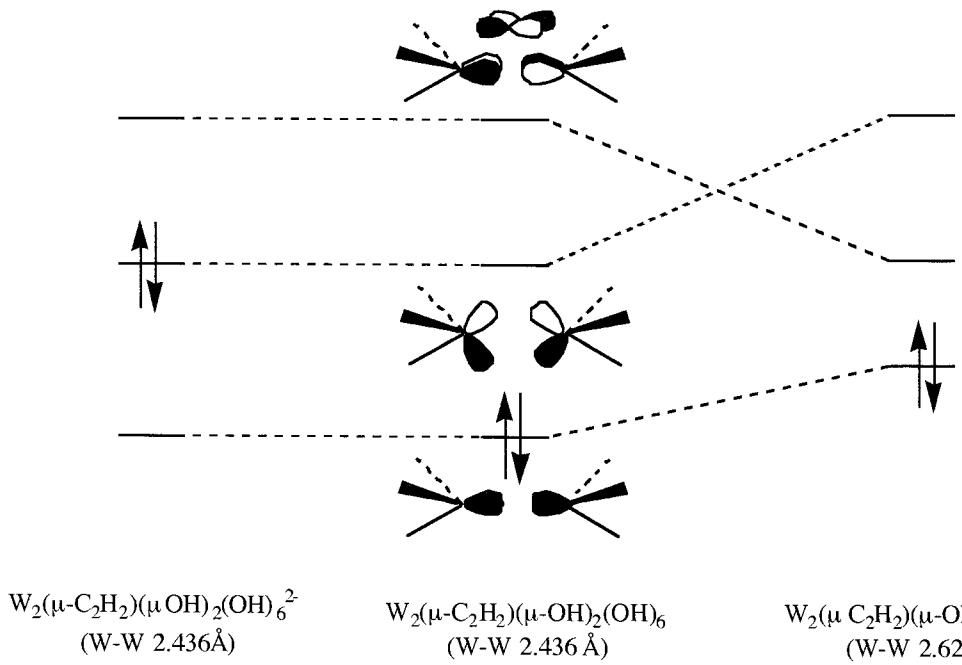

Fig. 12. Correlation diagram for the predicted molecular orbitals of $W_2(\mu\text{-}C_2H_2)(\mu\text{-}OH)_2(OH)_6^{2-}$ (W–W 2.436 Å), $W_2(\mu\text{-}C_2H_2)(\mu\text{-}OH)_2(OH)_6$ (W–W 2.436 Å), and $W_2(\mu\text{-}C_2H_2)(\mu\text{-}OH)_2(OH)_6$ (W–W 2.623 Å).

Table 1
Optimized values for RHF and Becke3LYP geometry optimizations of $W_2(\mu\text{-}C_2H_2)(\mu\text{-}OH)_2(OH)_6$. Estimated standard deviations from the crystal structure are provided in parentheses

Parameter	Actual	RHF (fixed bridging OH)	RHF (movable bridging OH)	Becke3LYP
W–W (Å)	2.6228 (8)	2.397	2.400	2.497
C–C (Å)	1.341 (16)	1.315	1.317	1.315
C–H (Å)	N/A	1.083	1.083	1.098
W–C (Å)	2.075 (11), 2.428 (12)	2.014, 2.303	2.010, 2.305	2.034, 2.393
$W\text{–}O_{bridging}$ (Å)	2.074 (7), 2.123 (7)	1.939	1.916, 1.963	1.872, 2.167
$W\text{–}O_{terminal}$ (Å)	1.920 (7)	1.761, 1.806, 1.829	1.763, 1.803, 1.830	1.781, 1.793, 1.831
$\angle_{C-C-H}$ (°)	N/A	135.8	135.5	137.9
$\angle_{W-W,C-C}$ (°)	63.4	66.7	66.3	61.0

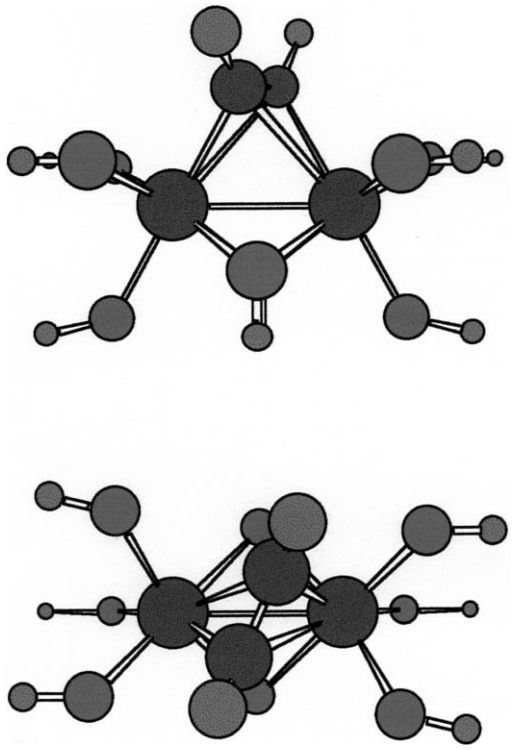

Fig. 13. Gaussian 92 RHF optimized structure for $W_2(\mu\text{-}C_2H_2)(\mu\text{-}OH)_2(OH)_6$.

Not surprisingly, the metal–metal bond distance is poorly calculated by all methods; the value obtained by the density functional calculation is closest to the crystallographically determined W–W bond length, but in all instances the calculated W–W distances are too short. However, the C–C bond distance found in these geometry optimizations approximates well the actual distance and the calculated C–C–H bond angle concurs with the notion that the triple bond of acetylene is well on its way to becoming a double bond upon coordination of the moiety to the metal centers. Other distances appear to be reasonably well calculated.

To test Hoffmann's suggestion that the displacement of the bridging ligands has little computational effect on the theoretically determined acetylene twist angle, an RHF optimization was performed in which the bridging alkoxides were constrained to be symmetrically bridging between the tungsten atoms. Various calculated structural parameters for this calculation are also given in Table 1. The acetylene positioned itself in nearly the same position as when the bridging alkoxides were not forced to be symmetrically bridging; the torsional angle was determined to be 66.7° as opposed to 66.3°.

5. Conclusion

Despite a difference of two metal-based electrons, the skewed orientation of the acetylene fragment in $W_2(\mu\text{-}NMe_2)_2(\mu\text{-}C_2Me_2)Cl_4(py)_2$ and $W_2(\mu\text{-}C_2H_2)(\mu\text{-}OH)_2(OH)_6$ is a result of the same valence molecular orbital interactions as found originally by Calhorda and Hoffmann. The LUMO of both complexes is a W–W π^*/δ^* and tungsten–acetylene bonding interaction, which is destabilized upon rotation of the C_2H_2 moiety. The HOMOs of the two complexes are different, but both are stabilized by similar metal–acetylene bonding interactions. The differences between the MO diagram proposed here for $W_2(\mu\text{-}C_2H_2)(\mu\text{-}OH)_2(OH)_6$ and that suggested by Calhorda and Hoffmann are due to the change in W–W bond order and subsequent difference in metal–metal bond length of these two complexes.

Our explanation also agrees with that of Mountford, who noted that in the second-order Jahn–Teller distorted alkyne complexes, the $M_2\text{-}\pi^*$ bonding level is either vacant or half-occupied such that the so-called electronic brake on distortion is released. Essentially, this argument does not require that the HOMO and LUMO of a given complex possess the same symmetry upon rotation of the acetylene fragment. Rather, with no metal-to-acetylene π^* molecular orbitals occupied at a torsional angle of 0° or 90°, the acetylene fragment rotates to make best use of the metal–metal bonding orbitals that are occupied. In the present case, there is only one metal–metal bond that is occupied, the W–W σ bond, which can π donate to the C_2H_2 unit via the tori of the d_{z2} atomic orbitals of which it is composed.

Finally, Gaussian 92 geometry optimizations lend credence to the belief that the skewed orientation of the C_2H_2 unit is due to metal–acetylene bonding interactions (i.e., a second-order Jahn–Teller distortion) rather than steric constraints imposed by bulky attendant ligands.

References

[1] T. Albright, M.H. Whangbo, J.K. Burdett, Orbital Interactions in Chemistry, Wiley Interscience, New York, 1985.
[2] R. Hoffmann, Angew. Chem. Int. Ed. Engl. 21 (1982) 711.
[3] M.H. Chisholm, D.L. Clark, M.J. Hampden-Smith, D.M. Hoffman, Angew. Chem. Int. Ed. Engl. 28 (1989) 432.
[4] J. Takats, Polyhedron 7 (1988) 931, and references therein.
[5] R.M. Bullock, T.J. Hembare, J.R. Norton, J. Am. Chem. Soc. 110 (1989) 7868.
[6] R.J. Hembre, C.P. Scott, J.R. Norton, J. Am. Chem. Soc. 109 (1987) 3468.
[7] M.H. Chisholm, K. Folting, M.A. Lynn, W.E. Streib, D.B. Tiedtke, Angew. Chem. Int. Edit. Engl. 36 (1997) 52.
[8] R.F. Fenske, M.B. Hall, Inorg. Chem. 11 (1972) 768.
[9] B.E. Bursten, J.R. Jensen, R.F. Fenske, J. Chem. Phys. 68 (1978) 3320.
[10] C. Mealli, D.M. Proserpio, J. Chem. Ed. 67 (1990) 399.
[11] M.J. Frisch, G.W. Trucks, H.B. Schlegel, P.M.W. Gill, B.G. Johnson, M.W. Wong, J.B. Foresman, M.A. Robb, M. Head-Gordon, E.S. Replogle, R. Gomperts, J.L. Andres, K. Raghavachari, J.S. Binkley, C. Gonzalez, R.L. Martin, D.J. Fox, D.J. Defrees, J. Baker, J.J.P. Stewart, J.A. Pople, Gaussian 92/DFT, Revision G.2, Gaussian, Pittsburgh, PA, 1993.

[12] R.B. Ross, J.M. Powers, T. Atashroo, W.C. Ermler, L.A. LaJohn, P.A. Christiansen, J. Chem. Phys. 93 (1990) 6654.
[13] T. Dunning, J. Chem. Phys. 53 (1970) 2823.
[14] S. Huzinaga, J. Chem. Phys. 42 (1965) 1293.
[15] D.M. Hoffman, R. Hoffmann, C.R. Fisel, J. Am. Chem. Soc. 104 (1982) 3858.
[16] K.J. Ahmed, M.H. Chisholm, J.C. Huffman, Organometallics 4 (1985) 1312.
[17] M.J. Calhorda, R. Hoffmann, Organometallics 5 (1986) 2181.
[18] F.A. Cotton, X. Feng, Inorg. Chem. 29 (1990) 3187.
[19] R.P. Aggarwal, N.G. Connelly, M.C. Crespo, B.J. Dunne, P.M. Hopkins, A.G. Orpen, J. Chem. Soc., Dalton Trans. (1992) 655.
[20] D.L. Thorn, R. Hoffmann, Inorg. Chem. 17 (1978) 126.
[21] S.G. Bott, D.L. Clark, M.L.H. Green, P. Mountford, J. Chem. Soc., Dalton Trans. (1991) 471.
[22] P. Mountford, J. Chem. Soc., Dalton Trans. (1994) 1843.